RSC Advances

PAPER

View Article Online
View Journal | View Issue

Cite this: *RSC Adv.*, 2021, **11**, 20370

Metal citrate nanoparticles: a robust water-soluble plant micronutrient source†

K. S. V. Poorna Chandrika,[ab] Dinabandhu Patra,[a] Praduman Yadav,[b] A. Aziz Qureshi[b] and Balaji Gopalan *[a]

A series of iron (Fe) and zinc (Zn) plant nanonutrients in citrate form were prepared by an eco-friendly solid-state grinding of the respective nitrates and citric acid. Ball-milling of the as-prepared Fe and Zn citrates resulted in nanosize particles. The as-prepared and ball-milled Fe and Zn citrates were characterized using Fourier-transform infrared spectroscopy (FTIR), thermogravimetric analysis and differential thermal analysis (TGA/DTA), and powder X-ray diffraction (XRD). The particle size and morphology of the obtained samples were studied using a scanning electron microscope (SEM) and transmission electron microscope (TEM). The obtained nanosized Fe and Zn citrates were analyzed for their plant uptake in the test crop soybean (var. JS-335) using the white-sand technique. The concentration of nutrients was estimated by atomic absorption spectrometry (AAS). A significant increase in nutrient absorption was observed in 6 h ball-milled samples of both Fe (789.8 μg per g of dry weight) and Zn (443.8 μg per g of dry weight) citrates. Such an increased nutrient absorption is due to the high mobility of nanocitrates. Therefore, nanocitrates can serve as an excellent source of plant nutrients in agriculture.

Received 14th April 2021
Accepted 24th May 2021

DOI: 10.1039/d1ra02907j

rsc.li/rsc-advances

Introduction

The increasing world population has forced the agricultural sector to increase crop productivity. The low productivity in most of the cropping systems, among other things, is due to imbalanced plant nutrition. The imbalanced use of chemical fertilizers increases crop production but disturbs the soil mineral balance and decreases soil fertility. Balanced nutrition, including secondary, micro and nitrogen, phosphorus, and potassium (NPK), has resulted in higher productivity, quality, and nutrient use efficiency (NUE). In the present agriculture system, micronutrients and secondary nutrients are crucial inputs in achieving the desired level of growth and yield.[1] Their deficiency causes a considerable decline in yield and quality. A lot of nutrient deficiency in the case of micronutrients has resulted in significant economic loss.[2] The essential agricultural soils of the world are deficient in zinc (Zn)-49%, boron (B)-31%, molybdenum (Mo)-15%, copper (Cu)-14%, manganese (Mn)-10%, and iron (Fe)-3%.[3] In this area, correcting the micronutrient deficiency as per the soil test values requires the application of large-scale micronutrients. As a result, the production costs increase, besides the irreparable damage to the soil structure, mineral cycles, soil microbial flora, and plants and leading to heritable mutations in future generations of consumers through the food chain.

Micronutrients like iron (Fe) and zinc (Zn) must be sufficient in the plant micro-environment. Fe and Zn are essential trace elements that help in plant growth as well as significant high yield. The Fe and Zn micronutrients also improve soil productivity.[3] Several crops respond to both soil and foliar applications of these two micronutrients. Any deficiency of these two micronutrients results in severe crop losses due to the lack of proper metabolic activities in which these two are involved.[4] Around the world, various Fe and Zn fertilizers such as sulfates, chlorides, oxides, and nitrates are used for soil or foliar applications. The dissolution of Fe and Zn oxides requires a specific reagent to get it dissolved. Such kind of reagent-specific solubility is complicated in case of plant nutrient application. The sulfate, chloride, and nitrate fertilizers are the most effective and quick solutions for the correction of Fe and Zn deficiency in crops.[5] Depending upon the crop, iron and zinc fertilizers are being used at the rate of 25–50 kg per ha as a basal dose.[6,7] But, the absorption rate ranges from 50–500 g per ha, and its use efficiency is accounting for 1–2 percent depending upon the crop.

The lesser absorption rate and use efficiencies are due to the fixation in soils, leaching, conversion into insoluble forms, precipitation, and immobilization. Due to the lesser use efficiency of soil-applied Fe and Zn micronutrients, foliar application of micronutrients is being utilized to correct deficiencies caused at different stages of crop.[8] The foliar-applied Fe and Zn nutrient's use-efficiency is less than 1%.

[a]*Department of Chemistry, Birla Institute of Technology and Science (BITS) Pilani, Hyderabad Campus, Jawahar Nagar, Kapra Mandal, Hyderabad, 500078, India. E-mail: gbalaji@hyderabad.bits-pilani.ac.in*

[b]*Crop Production Section, ICAR-Indian Institute of Oilseeds Research, Rajendranagar, Hyderabad, 500030, India*

† Electronic supplementary information (ESI) available. See DOI: 10.1039/d1ra02907j

These severe bottlenecks require larger quantities, which causes an environmental burden.[9] Later on, to overcome the above-said problems, chelate-based Fe and Zn micronutrients in the form of Fe/Zn–EDTA, Fe/Zn–EDDHA are most commonly used. The chelate fertilizers convert nutrients into a soluble form and enhance nutrient absorption by plants.[10] Few reports indicate that chelate-based nutrients through foliar and soil application increased the translocation of nutrients to all plant parts.[11,12] However, these compounds could not raise the absorption rate and use efficiency due to their ineffectiveness and causing severe pollution to the environment and human being through the food chain.[13,14] The chelates belong to the group consisting of citric acid, oxalic acid, tartaric acid, and boric acid. These chelates are successful in soil application which helps in mobilize nutrients and a slight improvement in use efficiency (2–4%); these chelates are eco-friendly due to several plant physiological and metabolic cycles.[15,16] Still, a need exists to improve the absorption by adopting newer approaches for micronutrient-based chelate compounds to deliver better.

Nanoscience has come as an era for its low cost and higher efficiency across various fields and its unique role in agriculture. Nanofertilizers are nutrient carriers less than 100 nm that can hold bountiful nutrient ions due to their high surface-to-volume ratio. Also, to commensurate with crop demand, nanofertilizers release the nutrients slowly and steadily.[17] Subramanian *et al.*[18] used nanofertilizers to control the release of nutrients from the fertilizer granules to improve the NUE while preventing the nutrient ions from either getting fixed or lost in the environment. Nanofertilizers in the form of nanoparticles have gained importance due to preparation methods and easy ways of application.[19] There are severe bottlenecks in the usage of nanoparticles: aggregation, toxicity in the environment, steric hindrance, secondary problems for human beings. As a result, the application of nanoparticles has been restricted in several countries.[20] Thus, the search for greener materials that plants can readily absorb without any bottleneck needs to be prioritized.[21] The chelates in nanosystem form will be advantageous to plant.[22]

The nanomaterials are synthesized by using toxic compounds, which are also expensive. There is also a requirement for high temperature and pressure, leading to a shift of research focus on developing greener methods for a sustainable environment.[23] Several greener methods have been reported to synthesize nanoparticles using biological materials like plant extracts as precursors.[24] Ball-milling process is one of the greener options with several advantages: high purity of ground products, low-temperature, controllable, reproducible, and cost-effective.[25–27] There has been a growing demand and awareness on designing eco-friendly chemical processes and products. The minimization of hazardous substances, adopting greener techniques and resources for safer and beneficial output material is sustainable. In general, the coarse metal citrate particles can be prepared by precipitating from an aqueous solution. In this context, our work focuses on using an eco-friendly solid-state grinding method followed by ball-milling of citrate-based Fe and Zn nanosystems (nano chelated Fe and Zn) for plant uptake.

Materials and methods

Ferric nitrate hydrous (FN; ($(Fe(NO_3)_3)\cdot 9H_2O$)) purity of 98%, zinc nitrate hydrous (ZN; ($Zn(NO_3)_2\cdot 6H_2O$)) purity of 98%, citric acid anhydrous (CA; ($C_6H_8O_7$)) purity of 99% were purchased commercially from SRL, India. All the reagents were used as such without further purification.

Synthesis of iron (Fe) and zinc (Zn) based citrates

Ferric citrate (FC) ($C_6H_5FeO_7$) was prepared by a solid-state grinding technique employing a 1 : 1 molar ratio of solid ferric nitrate ($(Fe(NO_3)_3)\cdot 9H_2O$) and solid citric acid ($C_6H_8O_7$). A novel method preparation was followed, involving vigorous grinding (45 minutes) of both the reactants until complete nitric acid vapors (HNO_3) evolved out as per the reaction given in eqn (1). The obtained composition was allowed to dry completely in a hot air oven maintained at 80 °C. For zinc citrate (ZC) ($[C_6H_5O_7]_2Zn_3$), a similar procedure was followed by grinding a 1 : 3 molar ratio of solid zinc nitrate ($Zn(NO_3)_2\cdot 6H_2O$) and solid citric acid ($C_6H_8O_7$). The obtained dry citrates of respective metals (Fe and Zn) were used for further nanosystems development without further purification.

$$Fe(NO_3)_3\cdot 9H_2O + C_6H_8O_7 \rightarrow C_6H_5FeO_7 + 3HNO_3\uparrow + 9H_2O \quad (1)$$

$$3Zn(NO_3)_2\cdot 6H_2O + 2C_6H_8O_7 \rightarrow (C_6H_5O_7)_2Zn_3 + 6HNO_3\uparrow + 9H_2O \quad (2)$$

Synthesis of iron (Fe) and zinc (Zn) based nanocitrates

The optimized ferric citrate and zinc citrate prepared through solid-state grinding were used to develop nano-citrates through planetary ball-milling equipment with a cooling unit to provide temperatures of 2–10 °C (XQM-1-A, Changsha Tianchuang Powder Technology Co. Ltd, China). The obtained ferric citrate and zinc citrate were ball-milled for different milling durations of 2 h intervals up to 10 h. The ball-milling was performed with 1 mm zirconium balls in the ratio of 1 : 10 (sample: balls) at 300 rpm in a grinding jar, which is made up of zirconium oxide. The samples were labeled as FC-0 (0 h ball-milled) and BFC-*X* (*X* h ball-milled; $X = 2, 4, 6, 8$, and 10 h). And for zinc citrates, ZC-0 (0 h ball-milled) and BZC-*X* (*X* h ball-milled; $X = 2, 4, 6, 8$, and 10 h). All the ball-milled samples were used for further studies without any further purification.

Characterization of synthesized nanosystems

Density of Fe and Zn citrates. The densities of FC-0 and ZC-0 and the respective BFC-10 and BZC-10 samples were determined by tapping method as per ASTM methods.[28] It was determined by using a graduated specific gravity bottle. The initial powder was taken in the bottles of known volume (V in cm^3) by tapping method until no powder can fit further in the bottles. The fitted powders were weighed (m in g). The tapped density (d in g cm^{-3}) was calculated based on the equation:

$$d = m/V$$

Fourier transform infrared (FT-IR) analysis. FTIR was used to identify the functional groups and their changes in metal citrate formation during the grinding process. The IR was measured for the samples before and after ball milling. FTIR spectrum was recorded using Thermo scientific Nicolet iS50 instrument at room temperature for 64 scans. The resolution was 4 cm^{-1}, and a diamond ATR crystal was used with the peak value of 5.14 in transmittance mode in a wavenumber range 4000–500 cm^{-1}.

Diffuse reflectance spectroscopy (DRS) spectroscopy. The change in color after ball milling of BFC-10 and BZC-10 compared to FC-0 and ZC-0 was monitored by measuring reflectance using JASCO V-650, UV-Vis spectrophotometer with a wavelength range of 200–700 nm. The samples were loaded on a quartz plate. The standard $BaSO_4$ was used as a reference sample.

Scanning electron microscopy (SEM) analysis. SEM analysis was used to analyze particle morphology and was carried out using a field-emission scanning electron microscope (FE-SEM) (FEI, Apreo LoVAc). A small amount of citrate powders of Fe and Zn of both ball-milled and as-prepared were loaded onto carbon tapes. Then, the samples were Au sputtered to a thickness of 5–7 nm.

Transmission electron microscopy (TEM) analysis. TEM images were taken for Fe and Zn citrates of both ball-milled and as-prepared by using Hitachi-7500. TEM was done by dispersing samples (1 μg) in pure isopropanol of volume 1 mL and ultrasonication for 30 s. The dispersed sample was loaded on a Cu grid and dried for 12 h at 60 °C. The dried TEM grids were used for imaging.

X-Ray diffraction (XRD). X-Ray diffraction was used to investigate FC-0, ZC-0, BFC-10, BZC-10 sample formation, and the crystal structure. The XRD patterns were recorded using Rigaku ULTIMA-IV with Cu-Kα radiation ($\lambda = 1.541$ Å) in the 2θ range of 10–80° at a scan rate of 3° min^{-1}.

Thermal properties. Thermogravimetric analysis (TGA) and differential thermal analysis (DTA) were carried out on a Shimadzu DTG-60 instrument. These data were collected from 30 to 700 °C with the heating rate at 10 °C per min in a nitrogen atmosphere to analyze mass loss and decomposition temperature for FC-0, ZC-0, BFC-10, BZC-10 samples.

Table 1 Densities of Fe and Zn citrates

S. No	Treatment	Density (g cm^{-3})
1	FC-0	0.843
2	ZC-0	0.791
3	BFC-10	1.1
4	BZC-10	0.92

Evaluation of Fe and Zn citrates on seedling growth of soybean

Soybean (glycine max var. JS-335) seeds were used for plant growth and uptake studies. Soybean was grown in small pots in controlled conditions of seed incubator on 1 kg quartz or white sand (diameter of 0.3–0.55 mm). The white sand was soaked overnight in a nitric acid solution of 2% concentration and washed thoroughly with the Milli-Q water until the rinsed water attained neutral pH (6.5–7). The Fe treatments applied in the white sand were: control (no Fe), FC-0, BFC-2, BFC-4, BFC-6, BFC-8, BFC-10 were added at a rate of 0.008 mmol of Fe per kg of sand. Similarly, the Zn treatments applied in the white sand were: control (no Zn), ZC-0, BZC-2, BZC-4, BZC-6, BZC-8, BZC-10 were added at a rate of 0.004 mmol of Zn per kg of sand. The powder forms of Fe and Zn citrates were mixed in sand uniformly.

Initially, soybean seeds were surface sterilized with sodium hypochlorite solution of 0.4% for 60 s and then rinsed immediately with distilled water to protect seedlings from any kind of diseases. About 15 seeds of soybean were sown in pots and maintained in a seed incubator having a temperature of 27 ± 1 °C for 15 days. No visual symptoms of deficiency and toxicity of Fe and Zn were observed. The experiment was conducted in

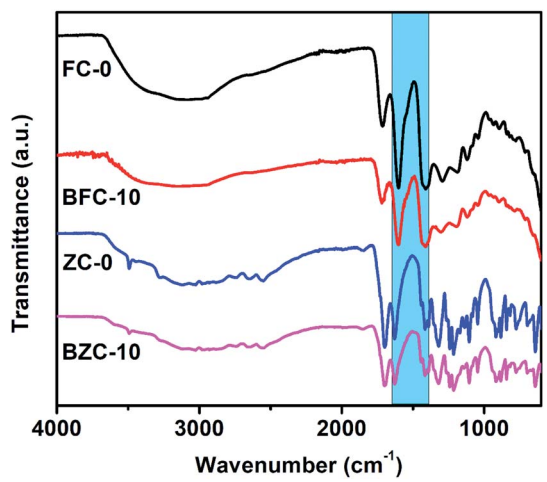

Fig. 1 FTIR spectra of ferric citrates (FC-0 and BFC-10) and zinc citrates (ZC-0 and BZC-10).

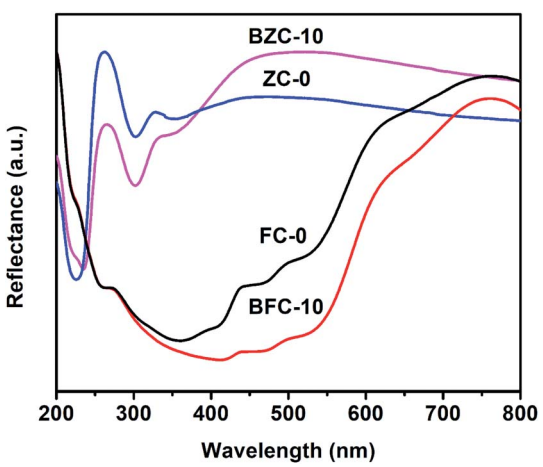

Fig. 2 UV-Vis spectra of ferric citrates (FC-0 and BFC-10) and zinc citrates (ZC-0 and BZC-10).

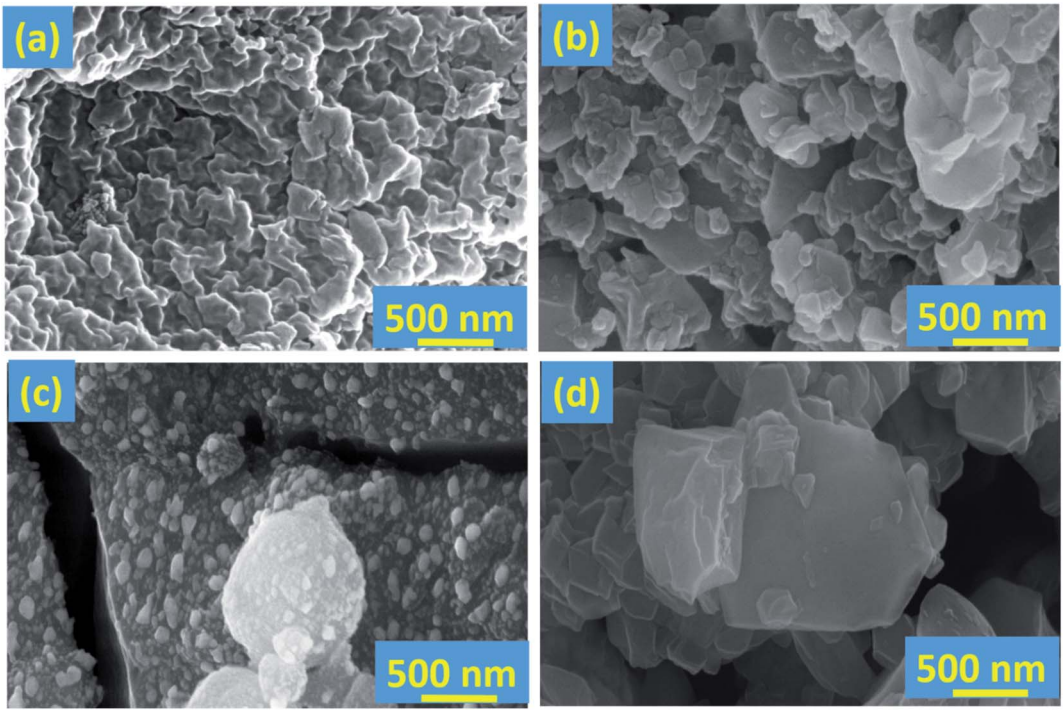

Fig. 3 SEM images of (a) FC-0; (b) ZC-0; (c) BFC-10; (d) BZC-10 samples.

triplicates. The seedlings were watered with an equal amount of deionized water based on the requirement in all treatments. At no stage, the added deionized water interfered with the test citrate samples. On the 16th day, the number of germinated seedlings were counted, rinsed thoroughly with deionized water, taken shoot and root length of each seedling. The seedlings were dried at 60–70 °C for 48 h for dry weight determination.

Atomic absorption spectrophotometer (AAS) analysis

For mineral analysis, the dried plant samples were grounded in pestle–mortar until the dry powder was obtained. After that, the sample (0.5 g) was digested using a 10 mL mixture of concentrated nitric acid and concentrated perchloric acid in the ratio of 9 : 1 on a hot plate having a temperature controller (JS Instruments, India) until clear and white fumes had resulted. After digestion, the digest filtrate was made up to 100 mL with deionized water. Then, appropriate dilutions were carried out to analyze Fe and Zn in the aliquots with AAS.

The atomic absorption spectrometer (PerkinElmer PinAAcle 900F, USA) was used to determine Fe and Zn with an air–acetylene flame. For Fe, the instrumental parameters employed were as follows: wavelength 248.3 nm; lamp current 12 mA; bandpass 0.2 nm; a hollow cathode lamp for the background correction. For Zn, the instrumental parameters were set as follows: wavelength 213 nm; lamp current 12 mA; bandpass 0.2 nm; a hollow cathode lamp for the background correction. The calibration graph was obtained by feeding working standards 0.5, 1.0, 2.0, and 3.0 mg L^{-1} for Fe and 0.2, 0.4, 0.6, and 0.8 mg L^{-1}, for Zn. Working standards for calibration were obtained by appropriate dilution of stock solution (1000 mg L^{-1}) of Fe and Zn (PerkinElmer Pure AAS Standards) using deionized water. The WINLAB 32 AA Version 7.4.1 software was used for final quantification.

Statistical data analysis

The analytical determination was carried out from the average mean data of 45 plants in a set (control and treated). All experimental data were expressed as mean of replicates and analyzed by the analysis of variance (ANOVA) using SPSS software 16.0 version.

Results and discussion

We have employed solid-state grinding of respective nitrates and citric acid in solid-state to prepare ferric citrate and zinc citrate samples. During the initial grinding stages, the reaction mixture turns to a liquid state due to water presence. On continuing the grinding process, the water content in the reaction mixture diminished, and nitric acid ceased to evolve. While the colors of ferric nitrate and citric acid were transparent brown and white, the ferric citrate color was reddish-orange. On continuous grinding for 10 min, the reddish-orange color of ferric citrate was visible, indicating the reaction completion. The effect of solid-state grinding on the citrate formation was investigated through FT-IR by doublet peak between 1600 and 1700 cm^{-1}. The citrates were analyzed for their purity through nitrate and citric acid estimation. The percentage of nitrates in the synthesized samples was to be 0.048%. This low percentage of nitrates implies that the added metal nitrates (wt% of nitrate is 23.9% in ferric nitrate and 22.3% in zinc nitrate) in the

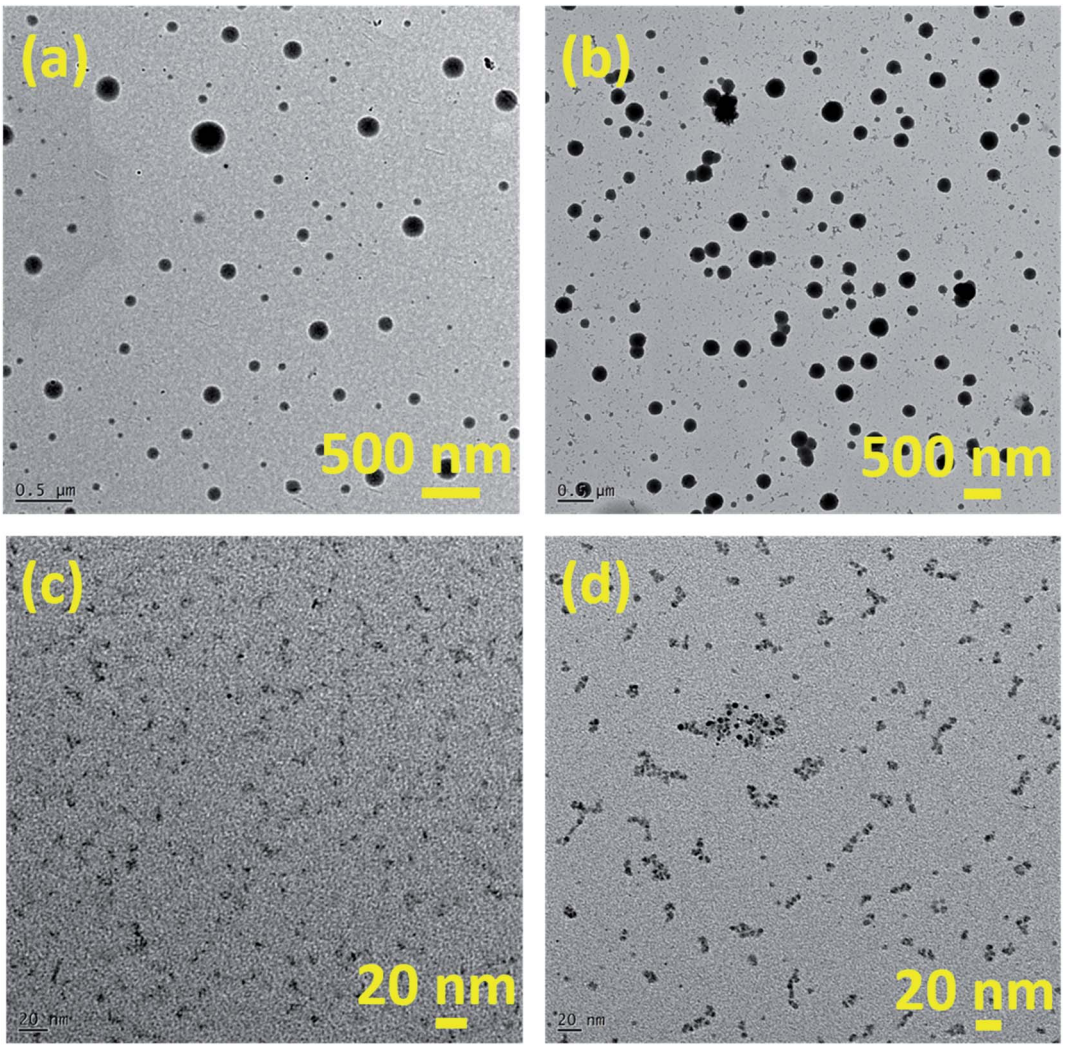

Fig. 4 TEM images of (a) FC-0; (b) ZC-0; (c) BFC-10; (d) BZC-10 samples.

respective reactions converted to metal citrates successfully. Typically, the nitrate stretching would be observed at 800 cm^{-1} in the IR spectroscopy. The absence of peak for nitrate in IR of FC-0 and ZC-0 samples confirms the reaction completion (Fig. 1 and S1†). Unreacted excess citric acid remained in small quantities in ZC-0 and FC-0 at the end of the solid-state grinding reaction. Even the excess citric acid does not cause any difference in plant uptake (Tables S1 and S2†). The formation of nanosize particles by ball milling of different durations was confirmed initially by color change (Fig. S1†) and further affirmed by SEM and TEM images.

Characterization of Fe and Zn citrates

FTIR analysis. The FTIR spectra of FC-0, ZC-0, BFC-10, and BZC-10 samples are shown in Fig. 1. The FTIR spectra of ferric nitrate and zinc nitrate are given in supplementary files (Fig. S2†). The FTIR spectra affirmed the coordination of both the metals Fe^{3+} and Zn^{2+} to their respective citrates and their ligand structures. There are not many differences observed in FTIR spectra of ball-milled Fe and Zn citrates. The characteristic bands at ~3493 cm^{-1}, 3025 cm^{-1} in ZC-0, and BZC-10; 3089 cm^{-1} in FC-0 and 3142 cm^{-1} in BFC-10 were assigned to O–H bond stretching. Two prominent peaks of vibrational stretches of ν_{asy} ($-COO^-$) and ν_{sy} ($-COO^-$) groups appeared at ~1601 and ~1409 cm^{-1} for FC-0; ~1603 and ~1413 cm^{-1} for BFC-10; ~1628 and ~1441 cm^{-1} for both ZC-0 and BZC-10. The difference in the values is ~200 cm^{-1}, which suggests that it is η^1-type bonding. The metal–oxygen peaks appeared in FC-0 (588 cm^{-1}), BFC-10 (590 cm^{-1}) and ZC-0 and BZC-10 at 578 cm^{-1}. For FC-0 and BFC-10, the presence of a peak at ~1720 suggests free –COOH groups. The FT-IR data confirms the successful formation of Fe and Zn citrates as reported.[29,30] It is worth mentioning that the molar ratio of zinc to citric acid is 1 : 3, and therefore, the features of citric acid would dominate in the ZC-0 and BZC-10 during their characterization.

Density of Fe and Zn citrate. The changes in densities of the Fe and Zn citrates after ball milling are shown in Table 1. The observed increase in density values for ball-milled samples compared to the respective as-prepared may be due to the smaller size and more compact structure.[31] Hence, the density increases with a reduction in particle size as more mass is constrained per unit volume.[32]

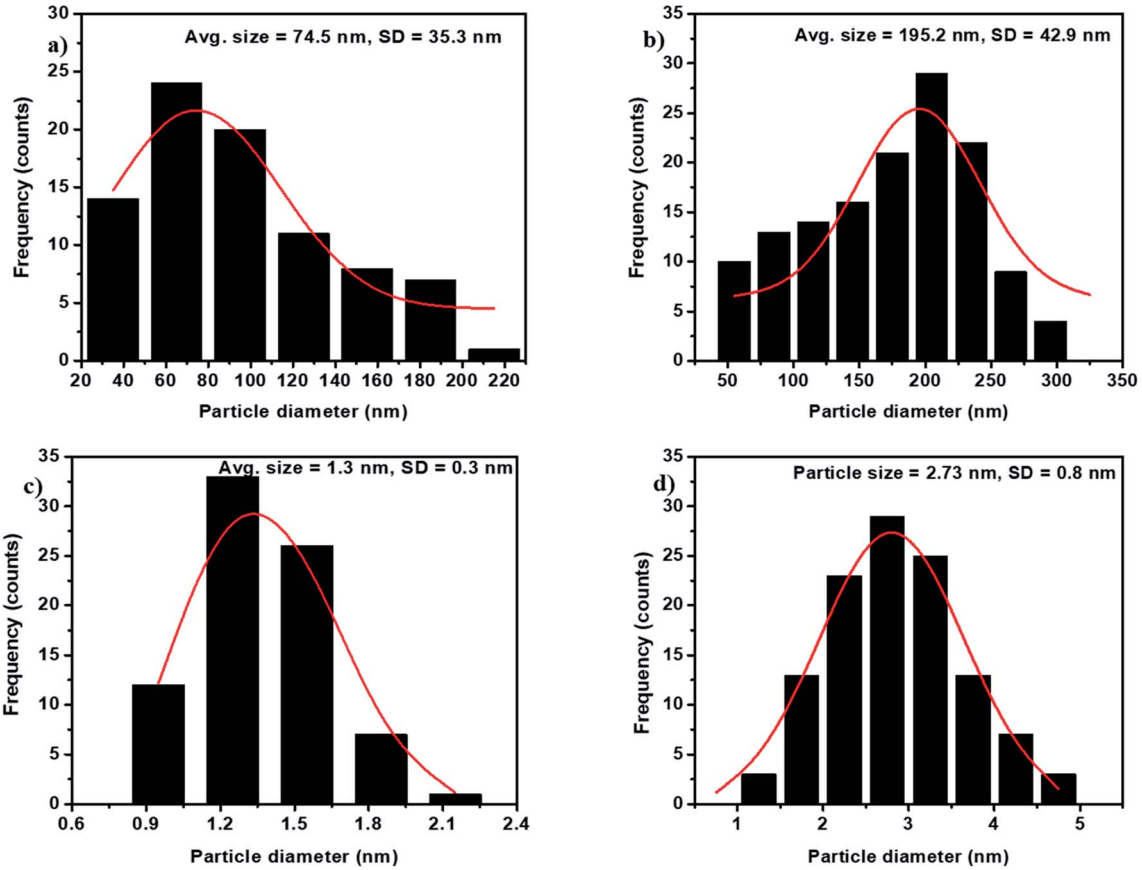

Fig. 5 Average particle sizes of (a) FC-0; (b) ZC-0; (c) BFC-10; (d) BZC-10 samples. Average particle sizes of (a) 74.5 ± 35.3 nm; (b) 195.2 ± 42.9 nm; (c) 1.3 ± 0.3 nm and (d) 2.73 ± 0.8 nm.

DRS spectroscopy. DRS spectra of as-prepared and ball-milled citrate samples of both Fe and Zn are shown (Fig. 2). The ZC-0 and BZC-10 are white-colored and showed a sharp increase in reflectance below 300 nm. Both FC-0 and BFC-10 showed reddish-orange color typical of commercial ferric citrate. Three IR bands were observed at 410, 470, and 539 nm. For BFC-10 and BZC-10 samples, there was a decrease in reflectance and a shift to higher wavelengths than its respective as-prepared samples. These observations could be due to the reduction in particle size due to ball milling. This study indicates that particle size reduction can be achieved by ball milling of Fe and Zn citrates.[33] The particle size reduction was further confirmed by electron microscope studies.

SEM and TEM analysis. The surface morphology and particle sizes of a Fe and Zn citrate prepared in this study were examined using SEM and TEM techniques. Fig. 3 and 4 show SEM and TEM images of the samples, respectively. The SEM images of FC-0 and ZC-0 indicate that the samples are aggregated and possess irregular morphology. There are smaller particles located on the bigger particles indicating a hierarchical structure present in the samples. The SEM images of ball-milled citrates (BFC-10 and BZC-10) in Fig. 3c and d show individual smaller particles and their ~70 nm size aggregates.[34] With an increase in milling duration, in both the samples, particle size decreased, and smaller particles aggregate into larger particles. Niasari *et al.*[26] and Arbain *et al.*[27] had reported similar results; during the synthesis of silica nanoparticles and iron oxide nanoparticles, the particle size reduced with the increase in milling duration. Even though aggregation was observed in SEM images, all particles are in nanoscale ranging from 1.5–5 nm, as observed in TEM images (Fig. 4 and 5). Since the molar ratio of zinc to citric acid is 1 : 3, the significant portion of TEM images may correspond to citric acid. The SEM and TEM analysis confirmed the formation of nanoparticles as a result of the ball-milling process.

X-Ray diffraction. X-Ray diffraction (XRD) patterns of the synthesized citrates are shown in Fig. S3.† The XRD pattern of FC-0 and BFC-10 did not show any peak, indicating the amorphous nature.[35] For ZC-0 and BZC-10, sharp peaks at 2θ values of 18.11°, 19.63°, 21.96°, 26.19°, 28.4°, 31.4°, 32.52°, and 36.79° were observed, indicating crystalline nature. However, all the peaks match with citric acid (JCPDS file no. 161157) as the mole ratio of zinc to citric acid 1 : 3, and therefore, the XRD pattern was indexed for citric acid.

Thermal properties. Fig. 6 shows the TGA plot of the as-prepared and ball-milled Fe and Zn citrates. Initially, the weight loss at 100 °C is due to the water loss in the samples. The weight loss in FC-0 and ZC-0 was 10% and 5%, respectively, indicating that the ferric citrate samples are more hygroscopic compared to zinc citrate. At the second stage, around 50%

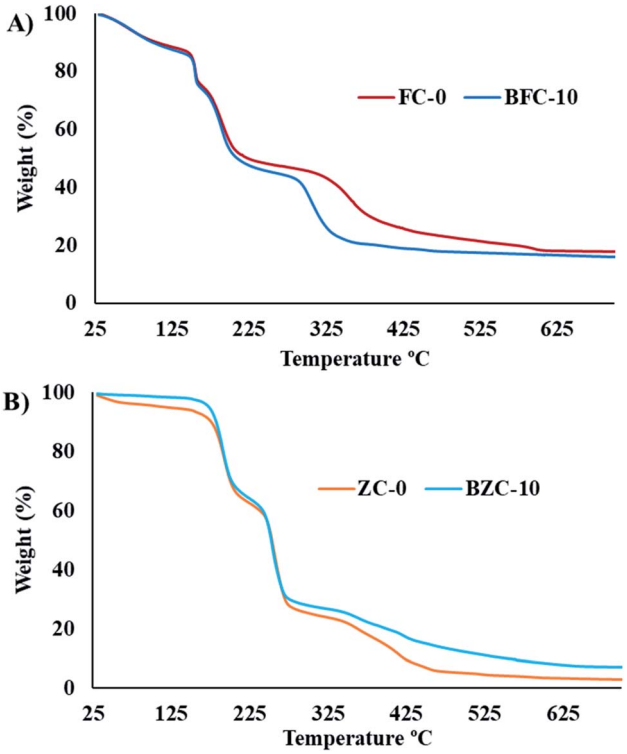

Fig. 6 TGA plots of (A) ferric citrates (FC-0 and BFC-10) and (B) zinc citrates (ZC-0 and BZC-10).

decomposition took place at temperature 223 °C for FC-0, 208 °C for BFC-10, and 253 °C for both ZC-0 and BZC-10. At 700 °C, the residual mass was 17.8% and 16.07%, respectively, for FC-0 and BFC-0. For ZC-0 and BZC-0, the residual mass was 2.72% and 7.07%, respectively. A minimal residual mass for ZC-0 and BZC-10 may be attributed to a small percentage of Zn in these samples. Not much difference in thermal decomposition pattern was observed for as prepared and ball-milled metal citrates except a reduction in the thermal decomposition temperature. This reduction implies no change in chemical composition but a change in the particle sizes due to ball-milling.[36]

Effect of plant uptake of nutrients on ball milling

The as-prepared ferric citrates and zinc citrates and the respective ball-milled samples were added to white sand tended to nutrient uptake (Table 2). The control sample experiments are also included. In ball-milled treated samples, an increase in nutrient uptake is observed in both Fe and Zn in comparison to as-prepared samples. Interestingly, a significantly higher nutrient uptake was observed in 6 h ball-milled samples of Fe (789.8 μg per g of dry wt) and Zn (443.8 μg per g of dry wt). The mineral nutrients uptake by plants from soil occurs majorly through plant roots. Several factors, soil type, soil composition, and soil chemistry influence the nutrient uptake efficiency mechanism. In roots, the changes like root elongation and root surface area will also occur to obtain nutrients from the soil. Thus, the changes in plant root structures occur for the allocation of nutrient resources. Such changes result in an increased root to shoot ratio in nutrient-limited plants.[37] Fig. 7 is a schematic representation of the experiment conducted in this study. Table 2 shows the summary of studies of nutrient intake by plants/seeds. A less root-to-shoot ratio in treated-sand than control-sand can be interpreted as root structure does not change, and nutrition acquisition in the plant is not majorly due to root elongation. The non-significant differences of root to shoot ratio between treatment and control is due to the experiment conducted in white sand, which is devoid of any kind of nutrients required for the plant. During watering, the care has been taken such that the deionized water used did not reach the nutrient application area.

Iron and zinc as-prepared ferric and zinc citrates used for plant growth, development, and uptake studies were without

Table 2 Plant uptake studies with developed metal citrates in soybean (var. JS-335)[a]

Treatment	Nutrient concentration of Fe μg per g of dry weight	Plant uptake of Fe μg per g of dry weight	Root to shoot ratio	Treatment	Nutrient concentration of Zn μg per g of dry weight	Plant uptake of Zn μg per g of dry weight	Root to shoot ratio
Control	295.8^{c}	—	0.25	Control	66.95^{c}	—	0.25
FC 1 : 1 0 hours	493.35^{b}	197.55	0.20	ZC 1 : 3 0 hours	288.95^{b}	222	0.19
BFC 1 : 1 2 hours	664.1 ^{ab}	368.3	0.17	BZC 1 : 3 2 hours	306^{b}	239.05	0.17
BFC 1 : 1 4 hours	662.95 ^{ab}	367.15	0.13	BZC 1 : 3 4 hours	311.2^{b}	244.25	0.23
BFC 1 : 1 6 hours	789.8^{a}	494	0.10	BZC 1 : 3 6 hours	443.85^{a}	376.9	0.17
BFC 1 : 1 8 hours	502.75^{b}	206.95	0.18	BZC 1 : 3 8 hours	353.7 ^{ab}	286.75	0.17
BFC 1 : 1 10 hours	534.15^{b}	238.35	0.20	BZC 1 : 3 10 hours	347.55 ^{ab}	280.6	0.22
CD (0.05)	173.5		NS	CD (0.05)	114.1		NS
CV	13.02		8.06	CV	15.9		11.3

[a] Means within a column followed by the same letters are not significantly different ($P < 0.0005$).

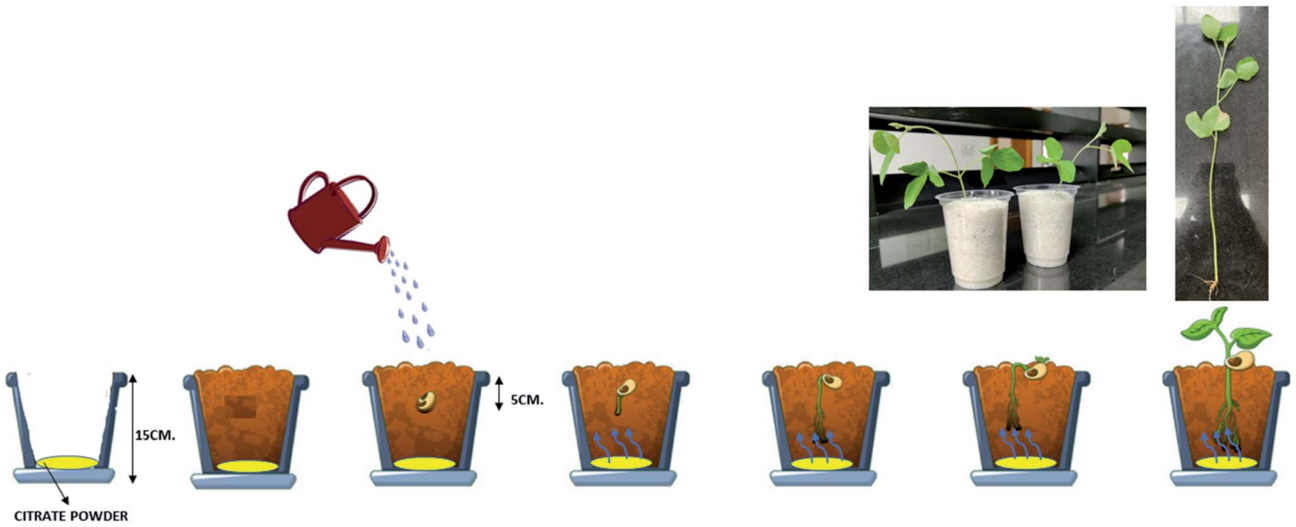

Fig. 7 Schematic presentation of plant uptake of metal citrates.

any symptoms. The results are reasonable compared to other reports under the given conditions and during the studied period.[38] For FC-0 and ZC-0 samples, the nutrient uptake was found to be 197.55 and 222 μg g^{-1} DW, respectively. The relatively higher uptake could be due to citric acid's chelation effect, which promotes nutrient mobilization. In general, uptake of nutrients in chelates will occur without the splitting of nutrients, which is thought to be a prerequisite for any nutrient absorption.[39,40] The uptake of the intact chelate or ligand-based nutrients improves physiological availability due to high cation exchange capacity.[1] In citric acid, it exists as citrate (deprotonated form) and forms mineral complexes with Al, Fe, Zn, Mn, Cu, and P in soil.[41–43] The citric acid also converts the insoluble form of minerals to soluble form by forming complexes and results in soil mobilization to make minerals available to plants.[44,45] In problematic soils, many plants exudate citric acid from its roots to enhance mineralization of insoluble forms and mobilization.[46,47] Even plants absorb citric acid through roots which is not entirely sufficient for mobilization of nutrients, so exogenous application of citric acid to soil microenvironment always results in beneficial and better mobilization of nutrients. The exogenous application of citric acid in problematic soils and increasing absorption of Ca^{2+}, K^{+}, Fe^{3+}, Zn^{2+} in studied crops like tomato, chickpea have been reported.[45,48]

It is evident that when the molar ratio of Fe: citric acid was 1 : 3, a higher uptake of 264.4 μg g^{-1} DW Fe was observed (Table S2†). Thus, the uptake of Fe and Zn could be attributed to citrates, which are ligated to the metal ions and aided by the interaction between citric acid and white-sand surface.

The ball-milled citrates showed an increased nutrient uptake compared to the as-prepared samples. For instance, the nutrient absorption values observed in BFC-6 and FC-0 were 494 and 197.55 μg g^{-1} DW, respectively. This difference in the absorption capacity may be attributed to the smaller particle size in the ball-milled samples (see Fig. 4). A similar trend was also observed in zinc systems. Diffusion is a phenomenon of transport in all directions, which results from the random movement of the particles. The average displacement of nanoparticles caused by the Brownian motion can be characterized by the diffusion coefficient D of the particle,[49] which can be related to particle mobility. The diffusion coefficient D depends on the temperature, matrix (effect of the interactions with the surrounding molecules), and particle size. Specifically, the D is inversely proportional to the diameter of the particles. The diffusion coefficient of nanoparticles as small as 100 nm in diameter will be twenty times higher than for the micron-sized molecules. The percentage of nutrient intake in BZC-6 is higher than that of BFC-6, which can be attributed to the excess citric acid, which aids the effective diffusion of Zn nutrient. However, BFC-10 and BZC-10 showed reduced nutrient uptake after 6 h of ball-milling, and this may be due to any kind of aggregation of particles, which needs to be confirmed in future studies. The Fe and Zn-based nanoparticles have resulted in reasonable nutrient absorption rates and improved chlorophyll content, biomass, plant growth, and overall yield in soybean crops.[8,50–52] For comparison, the nutrient uptake values reported in soybean for oxide nanoparticles of Fe and Zn are given in Table S3.† Nutrient absorption capacity is high in this reported study. The improved plant absorption of Fe and Zn could be due to the combined effect of (1) chelation for the mobilization of nutrients and (2) nano-effect to diffusion of particles into the plants. It can be correlated with previous studies on nanosystems of chelated nitrogen, calcium, iron in various crops like rice, sorghum, marigold, and apple.[22,50,52,53]

Conclusions

By employing solid-state grinding followed by ball-milling, we have prepared a series of Fe–citrate and Zn–citrate nanosystems. These nanosystems have been characterized by using various techniques. The obtained results demonstrated that the ball-mill treatment for different durations had influenced the

particle size of the Fe–citrate and Zn–citrates. But there was no change in crystallinity and room temperature stability of the citrates. The plant uptake of various duration ball-milled citrates has been influenced due to change in mobility behavior resulting in diffusion differences. The plant uptake study indicates the Fe and Zn nanocitrates potential as nutrients in agriculture for soil application purposes. The synthesis of citrates in nanosize was performed using a greener technique (solid-state grinding and followed by ball-milling) by minimizing hazardous materials, resulting in sustainability. These materials will be further explored for their uptake, use efficiency, synergistic and antagonistic activity under various conditions in our future studies.

Conflicts of interest

There are no conflicts to declare.

Acknowledgements

The authors thank Dr A. Vishnuvardhan Reddy, Former Director, ICAR-IIOR, and Central Analytical Lab, BITS-Pilani, Hyderabad Campus, for providing the facilities to carry out the work. The authors also gratefully acknowledge the financial support under the ICAR institute project (IIOR-104-17).

References

1 H. Marschner, *Mineral nutrition of higher plants*, Academic press, London, 2nd edn, 1995, p. 882.
2 S. S. Bhattacharya, G. N. Debkanta, C. Mandal and K. Majumdar, *Better Crops*, 2004, **88**(4), 52–57.
3 G. Melendi, P. Fernandez-Pacheo, R. Coronado, M. J. Corredor, E. Testillano, P. S. Risueno and M. C. Marquina, *Ann. Bot.*, 2008, **101**, 187–195.
4 G. Kalidasu, C. Sarada and T. Y. Reddy, *J. Spices Aromat. Crops.*, 2008, **17**(2), 187–189.
5 D. Suter, S. Banwart and W. Stumm, *Langmuir*, 1991, **7**, 809–813.
6 G. J. Patel, B. V. Ramakrishnayya and B. K. Patel, *Plant Soil*, 1977, **46**, 209–219.
7 J. P. Singh, R. E. Karamanos, N. G. Lewis and J. W. B. Stewart, *Can. J. Soil Sci.*, 1986, **66**, l83–187.
8 D. Alidoust and A. Isoda, *Acta Physiol. Plant.*, 2013, **35**, 3365–3375.
9 C. O. Dimkpa, D. E. Latta, J. E. McLean, D. W. Britt, M. I. Boyanov and A. J. Anderson, *Environ. Sci. Technol.*, 2013, **47**, 4734–4742.
10 H. Ghafari and J. Razmjoo, *Int. J. Agron. Plant Prod.*, 2013, **4**, 2997–3003.
11 F. M. Maas, D. A. M. Van de Wetering, M. L. Van Beusichem and H. F. Bienfait, *Plant Physiol.*, 1988, **87**, 167–171.
12 M. Ferrandon and A. Chamel, *Plant Physiol. Biochem.*, 1989, **27**, 713–722.
13 A. Hernandez, A. Garate and J. Lucena, *J. Plant Nutr.*, 1995, **18**, 1209–1223.
14 N. S. A. F. K. N. Karagiannidis, T. Thomidis, G. Zakinthinos and C. Tsipouridis, *Sci. Hortic.*, 2008, **118**(3), 212–217.
15 H. Marschner, V. Romheld and M. Kissel, *J. Plant Nutr.*, 1986, **9**, 695–713.
16 M. H. Nazaran, Chelate compounds, *US Pat.*, US8288587B2, 2012.
17 D. Lin and B. Xing, *Environ. Sci. Technol.*, 2008, **42**, 5580–5585.
18 K. S. Subramanian, C. Paulraj and S. Natarajan, Nanotechnological approaches in Nutrient Management, in *Nanotechnology Applications in Agriculture*, 2008, pp. 37–42.
19 M. Liu, R. Liang, F. Liu and A. Niu, *Polym. Adv. Technol.*, 2006, **17**, 430–438.
20 D. Alidoust and A. Isoda, *Environ. Earth Sci.*, 2014, **71**, 5173–5182.
21 M. Rui, C. Ma, Y. Hao, J. Guo, Y. Rui, X. Tang, Q. Zhao, X. Fan, Z. Zhang, T. Hou and S. Zhu, *Front. Plant Sci.*, 2016, **7**, 815.
22 S. Fakharzadeh, M. Hafizi, M. A. Baghaei, M. Etesami, M. Khayamzadeh, S. Kalanaky, M. E. Akbari and M. H. Nazaran, *Sci. Rep.*, 2020, **10**, 4351.
23 H. Herlekar, S. Barne and R. Kumar, *J. Nanoparticles*, 2014, 140614.
24 J. Y. Song and B. S. Kim, *Korean J. Chem. Eng.*, 2009, **25**, 808–811.
25 J. F. de Carvalho, S. N. de Medeiros, M. A. Morales, A. L. Dantas and A. S. Carricç, *Appl. Surf. Sci.*, 2013, **275**, 84–87.
26 M. S. Niasari, J. Javidi and M. Dadkhah, *Comb. Chem. High Throughput Screening*, 2013, **16**, 458–462.
27 R. Arbain, M. Othman and S. Palaniandy, *Miner. Eng.*, 2011, **24**, 1–9.
28 ASTM D7481-18, *Standard Test Methods for Determining Loose and Tapped Bulk Densities of Powders using a Graduated Cylinder*, ASTM International, West Conshohocken, PA, 2018.
29 M. Matzapetakis, C. P. Raptopoulou, A. Tsohos, V. Papaefthymiou, N. Moon and A. Salifoglou, *J. Am. Chem. Soc.*, 1998, **120**, 13266–13267.
30 H. Li and J. Su, *SF Journal of Material and Chemical Engineering*, 2018, **1**(1), 1008.
31 W. Yan, N. Li, Y. Li, G. Liu, B. Han and J. XU, *Bull. Mater. Sci.*, 2011, **34**(5), 1109–1112.
32 J. Sun, F. Zhang and J. Shen, *Mater. Lett.*, 2003, **57**, 3140–3148.
33 E. G. Goh, X. Xu and P. G. McCormick, *Scr. Mater.*, 2014, **78**, 49–52.
34 S. K. Chaudhuri and L. Malodia, *Appl. Nanosci.*, 2017, **7**, 501–512.
35 K. Ando, N. Manta, Iron (iii) citrate, substantially free of beta-iron hydroxide oxide, *US Pat.*, application no., 15/449132, 2012.
36 M. R. Sovizi, S. S. Hajimirsadeghi and B. Naderizadeh, *J. Hazard. Mater.*, 2009, **168**, 1134–1139.
37 B. J. Lopez, A. C. Ramirez and L. H. Estrella, *Curr. Opin. Plant Biol.*, 2003, **6**, 280–287.

38 K. Ylivainio, A. Jaakkola and R. Aksela, *J. Plant Nutr. Soil Sci.*, 2004, **167**, 602–608.
39 R. L. Chaney, J. C. Brown and T. LO, *Plant Physiol.*, 1972, **50**, 208–213.
40 H. Marschner, V. Romheld and M. Kissel, *Physiol. Plant.*, 1987, **71**, 157–162.
41 B. Campbell, *JAE*, 2010, **39**(1), 45–48.
42 H. Hu, C. Tang and Z. Rengel, *J. Plant Nutr.*, 2005, **28**(8), 1427–1439.
43 L. Shlizerman, K. Marsh, E. Blumwald and A. Sadk, *Physiol. Plant.*, 2007, **131**(1), 72–79.
44 Y. Wang, Y. He, H. Zhang, J. Schroder, C. Li and D. Zhou, *Soil Sci. Soc. Am. J.*, 2008, **72**(5), 1263–1268.
45 A. R. Sánchez-Rodríguez, M. C. del Campillo, J. Torrent and D. L. Jones, *J. Soil Sci. Plant Nutr.*, 2014, **14**(2), 292–303.
46 B. J. López, J. M. F. Nieto, R. V. Ramírez and E. L. Herrera, *Plant Sci.*, 2000, **160**(1), 1–13.
47 L. Palomo, N. Claassen and D. L. Jones, *Soil Biol. Biochem.*, 2006, **38**(4), 683–692.
48 L. Ström, A. G. Owen, D. L. Godbold and D. L. Jones, *Soil Biol. Biochem.*, 2005, **37**, 2046–2054.
49 F. Giorgi, D. Coglitore, J. M. Curran, D. Gilliland, P. Macko, M. Whelan, A. Worth and E. A. Patterson, *Sci. Rep.*, 2019, **9**, 12689.
50 J. R. Peralta-Videa, J. A. Hernandez-Viezcas, L. Zhao, B. C. Diaz, Y. Ge, J. H. Priester, P. A. Holden and J. L. Gardea-Torresdey, *Plant Physiol. Biochem.*, 2014, **80**, 128–135.
51 Y. Ge, J. H. Priester, L. C. Van De Werfhorst, S. L. Walker, R. M. Nisbet, Y. J. An, J. P. Schimel, J. L. Gardea-Torresdey and P. A. Holden, *Environ. Sci. Technol.*, 2014, **48**, 13489–13496.
52 M. Ghasemi Lemraski, G. Normohamadi, H. Madani, H. Heidari Sharif Abad and H. R. Mobasser, *Open J. Obstet. Gynecol.*, 2017, **7**, 591–603.
53 L. Amuamuha, A. Pirzad and H. Hashem Hadi, *Int. Res. J. Appl. Basic Sci.*, 2012, **3**(10), 2085–2090.